Acta Crystallographica Section D
Biological Crystallography
ISSN 0907-4449

Purification, crystallization and preliminary X-ray analysis of *Drosophila melanogaster* ferrochelatase

Kai-Fen Wang,[a]† Chia-Kuei Wu,[b]† Vera M. Sellers,[a] John P. Rose,[b] Bi-Cheng Wang[b] and Harry A. Dailey[a,b]*

[a]Department of Microbiology, Center for Metalloenzyme Studies, University of Georgia, Athens, GA 30602-7229, USA, and [b]Department of Biochemistry and Molecular Biology, Center for Metalloenzyme Studies, University of Georgia, Athens, GA 30602-7229, USA

† The first two authors contributed equally to this paper.

Correspondence e-mail: hdailey@arches.uga.edu

Received 23 November 1998
Accepted 4 March 1999

Ferrochelatase (protoheme ferrolyase, E.C. 4.99.1.1), the terminal enzyme in the heme biosynthetic pathway, catalyzes the insertion of ferrous iron into protoporphyrin IX to form protoheme. In eukaryotes, the protein is associated with the inner surface of the inner mitochondrial membrane, and in higher animals the enzyme contains a [2Fe–2S] cluster. This cluster is highly sensitive to NO and is coordinated by four Cys residues whose spacing in the primary sequence is unique. Ferrochelatase from *Drosophila melanogaster* has been expressed in *Escherichia coli* with an amino-terminal six-histidine tag and purified to homogeneity. The protein has been crystallized with the [2Fe–2S] cluster intact. The crystals belong to space group $I422$, with unit-cell dimensions $a = b = 158.1$, $c = 171.2$ Å and two molecules in the asymmetric unit, and diffract to 3.0 Å resolution.

1. Introduction

The enzyme ferrochelatase (E.C. 4.99.1.1) catalyzes the insertion of ferrous iron into protoporphyrin IX to form protoheme IX (heme). This enzyme is found in essentially all prokaryotes and eukaryotes, with the exception of those few organisms which either do not contain heme or obtain heme from a host organism. To date, over two dozen DNA sequences for ferrochelatase have been obtained although no Archael ferrochelatases have been reported. When characterized, the enzyme has been shown to utilize ferrous iron, zinc and divalent cobalt, except in *Bacillus subtilis* where divalent copper, but not cobalt, is used (Hansson & Hederstedt, 1994) and in *Azospirillum brasilense* where divalent nickel is also utilized (see Dailey, 1996). The divalent heavy-metal ions of lead, cadmium, manganese and mercury are competitive inhibitors of ferrochelatase (Dailey, 1988). Trivalent and monovalent metal ions have no effect on enzyme activity and are not substrates. For the porphyrin substrate IX isomers of porphyrin with vinyl, hydroxyethyl, ethyl or hydrogen as substituents at the 2,4 positions are acceptable.

With the exception of ferrochelatase from *B. subtilis*, which is a soluble protein (Hansson & Hederstedt, 1994), all are membrane-associated. In prokaryotes, ferrochelatase is usually associated with the cytoplasmic membrane (Dailey, 1990). In eukaryotes, it is nuclear-encoded and cytoplasmically synthesized, and the precursor form of the enzyme is translocated to the matrix side of the inner mitochondrial membrane in an energy-requiring step which also involves proteolytic processing of the protein to its mature size (Karr & Dailey, 1988). The eukaryotic enzymes possess an additional 30–50 amino-acid residues at the carboxyl terminus which are lacking in bacteria. The function of this extension is unknown, but its removal in yeast or animal ferrochelatase results in loss of enzyme activity (Dailey, Sellers *et al.*, 1994). In animal ferrochelatases, there exists a [2Fe–2S] cluster (Dailey, Finnegan *et al.*, 1994) which is coordinated by three Cys residues which are present in the carboxyl terminal 30-residue extension (Crouse *et al.*, 1996) and a fourth Cys residue located approximately 200 residues to the amino-terminal side of the second coordinating Cys residue (Sellers *et al.*, 1998). This cluster, which has a unique Cys–(x_{207})–Cys–(x_2)–Cys–(x_4)–Cys spacing, is very sensitive to NO *in vivo* and *in vitro* (Sellers *et al.*, 1996). This NO-sensitive cluster not only gives animal ferrochelatases a unique property, but also makes the protein considerably more thermolabile than the corresponding prokaryotic enzymes. The purpose and function of this NO-sensitive [2Fe–2S] cluster is unknown, but it has been suggested that it is involved in an immune response to infection *via* regulation of heme/iron homeostasis, since increased NO production by macrophages during an infection results in reduction of cellular heme synthesis and an increase in heme catabolism. Determination of the crystal structure for animal ferrochelatase may help to answer this question as well as to provide a basis for understanding the catalytic functioning of this protein.

The catalytic model for ferrochelatase was put forward over ten years ago and has slowly gathered experimental support (see Lavallee, 1988; Dailey, 1997). In this model, the enzyme is proposed to first bind ferrous iron and then porphyrin. Metallation is facilitated by enzyme-catalyzed porphyrin macrocycle distortion. Metal insertion results in the formation of protoheme, which is released as a planar moiety. Data in support of this model involve thermodynamic consideration of metal insertion into a distorted macrocyclic porphyrin (Lavallee, 1988), tight-binding competitive inhibition of the enzyme by *N*-alkylporphyrins (as transition-state analogs; Dailey & Fleming, 1983), catalytic antibodies which mimic the ferrochelatase reaction (Cochran & Schultz, 1990) and, most recently, resonance Raman studies on porphyrin bound to ferrochelatase (Blackwood *et al.*, 1997).

Recently, the crystal structure of ferrochelatase from the bacterium *B. subtilis* was published (Al-Karadaghi *et al.*, 1997). This structure, while representing a landmark for ferrochelatase research, revealed little about the potential catalytically important residues in the putative active-site region, since no substrate-bound or product-bound forms of the protein were crystallized. In addition this protein, unlike other ferrochelatases, does not appear to be membrane-associated and its metal-utilization profile is unique among known ferrochelatases. As a bacterial ferrochelatase, it also lacks the carboxyl-terminal extension and [2Fe–2S] cluster. Finally, a significant helix–loop–helix region which appears to be part of, or adjacent to, the putative active site, is in a region where the *B. subtilis* protein contains 14 fewer amino acids than are found in animal ferrochelatases. Overall, the *B. subtilis* and human ferrochelatases are only 12% identical. Thus, in order to understand the animal ferrochelatases, it is necessary to obtain the crystal structure of one of these proteins.

During the course of our studies, we have expressed and characterized eukaryotic ferrochelatases from human (Dailey, Sellers *et al.*, 1994), mouse (Sellers & Dailey, 1997), chicken, frog (Day *et al.*, 1998), *Saccharomyces cerevisiae* (Eldridge & Dailey, 1992) and *Drosophila melanogaster* (Sellers *et al.*, 1998). While these are all highly similar, except for the lack of a [2Fe–2S] cluster in the *S. cerevisiae* enzyme, they possess distinct solubilities. It was found that the expressed *Drosophila* ferrochelatase with a His_6 tag yielded high-purity protein preparations which were more stable to storage and crystallization conditions than were the other proteins. Preliminary crystallographic studies on the *Drosophila* ferrochelatase are reported herein.

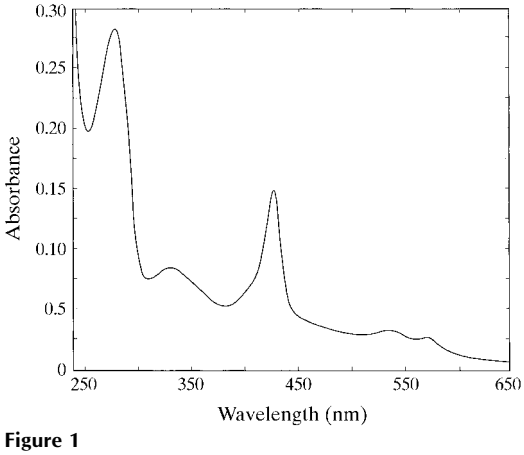

Figure 1
Ultraviolet–visible absorbance spectrum for purified *D. melanogaster* ferrochelatase. The spectrum was obtained after overnight dialysis of approximately 5 μ*M* protein and shows the presence of some residual bound protoporphyrin (absorbance maximum at 424 nm) and an intact [2Fe–2S] cluster.

2. Crystallization

Drosophila ferrochelatase cDNA was isolated using complementation of *Escherichia coli* Δhem H, a ferrochelatase-deficient strain (Miyamoto *et al.*, 1991), with a λ ZAP cDNA library (Stratagene Inc.). The cDNA encoding *Drosophila* ferrochelatase was amplified by PCR, with two primers which contain *Nco*I and *Bgl*II restriction sites at the 5′ and 3′ ends, respectively. For high levels of expression and simple purification, an expression vector containing a six-histidine terminal leader was constructed (Dailey & Dailey, 1996). The expression vector (pTDFc) was electroporated into *E. coli* strain JM 109. A single clone containing the pTDFc plasmid was inoculated into 100 ml Circlegrow (Bio 101) supplemented with 100 μg ml^{-1} ampicillin and grown with shaking at 310 K overnight. This 100 ml culture was used as an inoculum for 1 l of Circlegrow with ampicillin and incubated at 310 K for 20 h with shaking. Cells were harvested by centrifugation at 9000*g* for 15 min at 277 K and the cell pellet was suspended in 55 ml solubilization buffer [50 m*M* Tris–MOPS pH 8.0, 0.1 *M* KCl, 1.0%(*w*/*v*) sodium cholate]. The cell suspension was sonicated on ice for 3 × 30 s and centrifuged at 100000*g* for 45 min at 277 K. The supernatant was loaded onto a TALON matrix column (2 ml bed volume; Clontech, Palo Alto, CA) which had been equilibrated with solubilization buffer. The column was washed three times with 30 ml of the solubilization buffer before the *Drosophila* ferrochelatase was eluted with 10 ml of elution buffer [50 m*M* Tris–MOPS pH 8.0, 0.1 *M* KCl, 1.0%(*w*/*v*) sodium cholate, 200 m*M* imidazole]. The protein yield was approximately 20 mg per litre of culture. The utilization of the expressed His tag for purification of ferrochelatases does not affect the enzyme activity or stability, although it substantially increases the protein solubility. Enzyme produced without the His tag precipitated out of solution within a few hours and could not be crystallized. Fractions containing *Drosophila* ferrochelatase were dialyzed overnight against 2 l of 10 m*M* *N*-ethylmorpholine acetic acid buffer pH 8.0 at 277 K, concentrated to 45 mg ml^{-1} with a Biomax 10K concentrator (Millipore Corp, MA) and stored at 193 K. This exchange of buffer to put the protein into the *N*-ethylmorpholine acetate without added detergents was crucial to the subsequent crystallization. Without buffer exchange the protein would not crystallize. A variety of other buffers, both with and without added detergent, were tried and none resulted in crystal formation. Dialysis into most buffers resulted in protein precipitation.

SDS–polyacrylamide gel electrophoresis demonstrates a single protein band with a calculated molecular weight of approximately 42 kDa, which corresponds well with the molecular weight of 43032 Da predicted from the derived amino-acid sequence. The isolated *Drosophila* ferrochelatase has visible spectral features at 320 nm and broad features around 550 nm, which are characteristic of the [2Fe–2S] cluster present in this protein (Fig. 1), and has a calculated molar extinction coefficient of 55600 M^{-1} cm^{-1} at 278 nm. Also seen is an absorbance peak at 423 nm resulting from some residual protein-bound heme (enzyme product). It is not known if the crystal examined contained bound heme.

Hampton Crystal Screens I, II and MEMBFAC (Hampton Research, Laguna Hills CA) were used to screen for suitable crystallization conditions. Screening was performed at 277, 281 and 291 K using the hanging-drop vapor-diffusion technique. Drops (4 μl) contained equal volumes of protein concentrate and reservoir solution. The only detectable crystals observed in the initial screen were from a leaking well equilibrated at 291 K whose initial condi-

tions were 18% PEG 400 and 0.1 *M* ammonium sulfate in 0.1 *M* sodium HEPES buffer pH 7.5. After accounting for evaporation, these conditions were refined and larger crystals (0.1 × 0.1 × 0.15 mm) were obtained using a reservoir solution containing 32% PEG 400, 0.3 *M* ammonium sulfate, 0.04 *M* NaH_2PO_4 in 0.1 *M* sodium HEPES pH 7.5. These crystals were harvested, washed three times with 20% PEG 400, 0.3 *M* ammonium sulfate in 0.1 *M* sodium HEPES buffer pH 7.5 to remove any surface film covering the crystals, ground by sonication and used as seed crystals in new preparations. Crystals measuring 0.1 × 0.1 × 0.2 mm (Fig. 2) could be obtained at 281 K using seeded drops and a reservoir solution containing 29% PEG 400, 0.3 *M* ammonium sulfate, 0.04 *M* NaH_2PO_4 in 0.1 *M* sodium HEPES pH 7.5. Although the microseeding technique produced larger crystals, the crystals were always embedded in a gelatinous matrix which may be a limiting factor in crystal growth. Addition of detergents from the Hampton Research detergent screen kit had little effect on crystal size, which was unexpected as ferrochelatase is a membrane-associated protein which requires detergents for solubilization.

3. Space-group determination and data collection

For data collection, a crystal measuring 0.1 × 0.1 × 0.2 mm was mounted in a 0.2 mm rayon loop and flash-cooled to 100 K in a nitrogen-gas cold stream (Oxford Cryosystems Cryostream). A data set to 3.2 Å resolution was collected on a Bruker 2X2 Mosaic CCD detector at ID17 (IMCA-CAT), the Advanced Photon Source, Argonne National Laboratory, using the unfocused undulator beam. The data set consisted of 400 0.25° data frames, each exposed for 3 s.

The data were indexed, integrated and scaled using *HKL*2000 (Otwinowski & Minor, 1997) and yielded 16688 unique reflections (99% complete) with an average

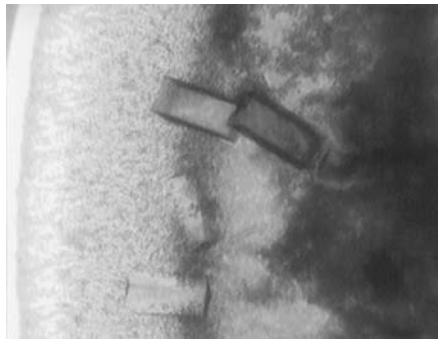

Figure 2
Crystals (0.1 × 0.1 × 0.2 mm) of *D. melanogaster* ferrochelatase.

$I/\sigma(I)$ of 6.11, reflecting the diffraction quality and size of the crystal used in the experiment. After scaling, $R_{\rm merge}$ for the data set was 0.14, which reflects the weak diffraction quality of the small crystal. The data indexed in a body-centered tetragonal lattice with $a = b = 158.1$ and $c = 171.2$ Å. Analysis of the three-dimensional diffraction pattern indicated that the space group was *I*422. Assuming two molecules per asymmetric unit, the Matthews coefficient (Matthews, 1968) is calculated to be 3.10 $Å^3\ Da^{-1}$, which corresponds to a solvent content of 58%, which is in the range typical for most protein crystals.

This work was supported by grants from the National Institutes of Health DK 32303 to HAD and the Georgia Research Alliance to B-CW. Use of the Advanced Photon Source was supported by the US Department of Energy, Basic Energy Sciences, Office of Energy Research, under contract No. W-31-109-Eng-38. Data were collected at beamline 17-ID using the facilities of the Industrial Macromacular Crystallography Association Collaboration Access Team (IMCA-CAT) at the Advanced Photon Source. These facilities are supported by the companies of the Industrial Macromolecular Crystallography Association through a contract with Illinois Institute of Technology (IIT) executed through the IIT's Center for Synchrotron Radiation Research and Instrumentation.

References

Al-Karadaghi, S., Hansson, M., Nikonov, S., Jönsson, B. & Hederstedt, L. (1997). *Structure*, **5**, 1501–1510.
Blackwood, M. E. Jr, Rush, T. III, Medlock, A., Dailey, H. A. & Spiro, T. G. (1997). *J. Am. Chem. Soc.* **119**, 12170–12174.
Cochran, A. G. & Schultz, P. G. (1990). *Science*, **249**, 781–783.
Crouse, B., Sellers, V. M., Finnegan, M. G., Dailey, H. A. & Johnson, M. J. (1996). *Biochemistry*, **35**, 16222–16229.
Dailey, H. A. (1988). *NY Acad. Sci.* **514**, 81–86.
Dailey, H. A. (1990). Editor. *Biosynthesis of Heme and Chlorophylls*, pp. 123–162. New York: McGraw–Hill.
Dailey, H. A. (1996). *Mechanisms of Metallocenter Assembly*, edited by G. L. Eichorn, L. G. Marzilli & R. P. Hausinger, pp. 77–98. New York: VCH.
Dailey, H. A. (1997). *J. Biol. Inorg. Chem.* **2**, 411–417.
Dailey, H. A., Finnegan, M. G. & Johnson, M. K. (1994). *Biochemistry*, **33**, 403–407.
Dailey, H. A. & Fleming, J. E. (1983). *J. Biol. Chem.* **258**, 11453–11459.
Dailey, H. A., Sellers, V. M. & Dailey, T. A. (1994). *J. Biol. Chem.* **269**, 390–395.
Dailey, T. A. & Dailey, H. A. (1996). *Protein Sci.* **5**, 98–105.
Day, A. L., Parsons, B. M. & Dailey, H. A. (1998). *Arch. Biochem. Biophys.* **359**, 160–169.
Eldridge, M. G. & Dailey, H. A. (1992). *Protein Sci.* **1**, 271–277.
Hansson, M. & Hederstedt, L. (1994). *Eur. J. Biochem.* **220**, 201–208.
Karr, S. R. & Dailey, H. A. (1988). *Biochem. J.* **254**, 799–803.
Lavallee, D. K. (1988). *Mechanistic Principles of Enzyme Activity*, edited by J. F. Liebman & A. Greenberg, pp. 77–98. New York: VCH.
Matthews, B. M. (1968). *J. Mol. Biol.* **33**, 491–497.
Miyamoto, K., Nakahigashi, K., Nishimura, K. & Inokuchi, H. (1991). *J. Mol. Biol.* **219**, 393–398.
Otwinowski, Z. & Minor, W. (1997). *Methods Enzymol.* **276**, 307–326.
Sellers, V. M. & Dailey, H. A. (1997). *Methods Enzymol.* **281**, 378–387.
Sellers, V. M., Johnson, M. J. & Dailey, H. A. (1996). *Biochemistry*, **35**, 2699–2704.
Sellers, V. M., Wang, K.-F., Johnson, M. K. & Dailey, H. A. (1998). *J. Biol. Chem.* **273**, 22311–22316.